PERMEABILITY AND COMPACTION CHARACTERIZATION OF A 3D ORTHOGONAL FABRIC USING IN-SITU µXCT

M. A. Ali*[1], R. Umer[1, 2], K. A. Khan[1]

[1]*Department of Aerospace Engineering, Khalifa University of Science and Technology, Abu Dhabi, UAE*
[2]*Centre for Future Materials, University of Southern Queensland, Toowoomba, Queensland, 4350 Australia.*
*Corresponding author (muhammad.ali@kustar.ac.ae)

Keywords: *Liquid composite moulding; Permeability; Compaction Response; In-situ micro CT; 3D fabrics;*

Introduction

In Liquid composite moulding (LCM) process characterization and optimization, it is important to know the preform compaction and permeability characteristics, which involve costly, time consuming and tedious experimental and modelling procedures [1, 2]. Preform permeability knowledge is needed a-priori for mould filling simulations and process optimization. The analytical models are limited to very simplified cases. Hence, many researchers are relying on time and labour intensive measurements obtained from experiments, employing a number of pressure sensors, flowmeters, optical devices etc. [3]. Numerical simulations using commercial Computational Fluid Dynamics (CFD) software or in-house computer codes are also used to obtain the preform permeability. Numerical permeability computation procedures use geometric modelling of the reinforcements that do not always capture the real architecture as well as the deformations associated with the compaction process. Nevertheless, these modelling approaches do not capture the real-time compaction of the reinforcements [4]. Here, we proposed an efficient in-situ non-destructive characterization and computational framework using X-ray micro computed tomography (µXCT) with an ability to extract information that yield simultaneously the compaction responses and permeability values of a reinforcement. The method proposed here is applied to compute the permeability in the principle directions and obtain the compaction behaviour of a 3D orthogonal fabric.

Materials and Methods

An orthogonal 3D fabric supplied by Sigmatex, UK, was investigated in this study. The experimental setup consists of DEBEN CT5000 in-situ testing stage and GE Nanotom CT machine. The µXCT images with a voxel size of 25 µm are reconstructed as a 3D voxel based computational model on which numerical flow simulation is performed in the FlowDict module of GeoDict. For the permeability computation, only inter yarn flow is considered. The flow simulation is based on the Stoke's equations given as

$$\boldsymbol{\nabla} . \boldsymbol{v} = \mathbf{0} \tag{1}$$

$$\mu \boldsymbol{\nabla}^{\mathbf{2}} \boldsymbol{v} - \boldsymbol{\nabla} P = \mathbf{0} \tag{2}$$

where $\boldsymbol{v}$ is the velocity vector, $\boldsymbol{\mu}$ is the fluid viscosity an P is the fluid pressure. The permeability $\boldsymbol{K}$ of the preform with porosity ϕ is then calculated from the volume averaged velocity $\langle \boldsymbol{v} \rangle$ using Darcy's law given as,

$$\boldsymbol{K} = \phi \langle \boldsymbol{v} \rangle \frac{\mu}{\boldsymbol{\nabla} P} \tag{3}$$

Preliminary Results and Discussion

Figure 1 shows the velocity distributions for flow in all directions at the initial thickness. The flow fields suggest the resin is forced to follow a tortuous path through the preform because of intricate preform architecture, and there are well connected flow paths in three dimensions. The flow paths are interrupted by the z-binder for the in-plane flows (Figure 1 (a) and (b)) whereas in case of transverse flow, dominant flow is present around the binder fibre. It has been observed that these flow channels become disconnected and shrink in size upon compaction.

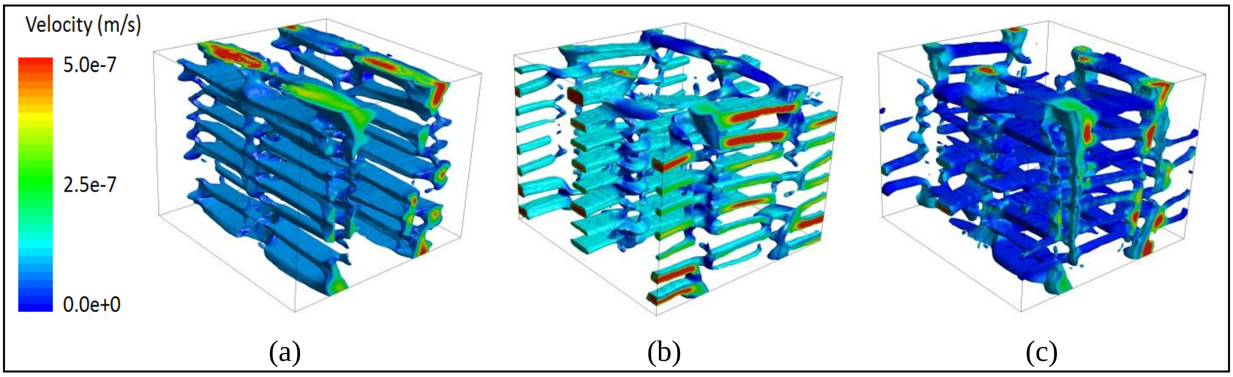

Figure 1: *Flow fields in the principle directions (a) K_{11}, (b) K_{22} and (c) K_{33} at the initial thickness.*

The compaction behavior of the test fabric is summarize as a stress relaxation curve shown in Figure 2 (a). At each compaction level, once the stress reaches the peak value, it drops instantaneously and relaxes to a stable value until there is no further visible drop [5]. Under the applied stress, the inter yarn gaps reduces as shown in the inset of Figure 1 (a). The computed permeability values are plotted in Figure 2 (b) as a function of the fiber volume fraction, along with the experimental data [6]. This figure indicates that the drop in K_{33} with increasing V_f was significant for the 3D fabric.

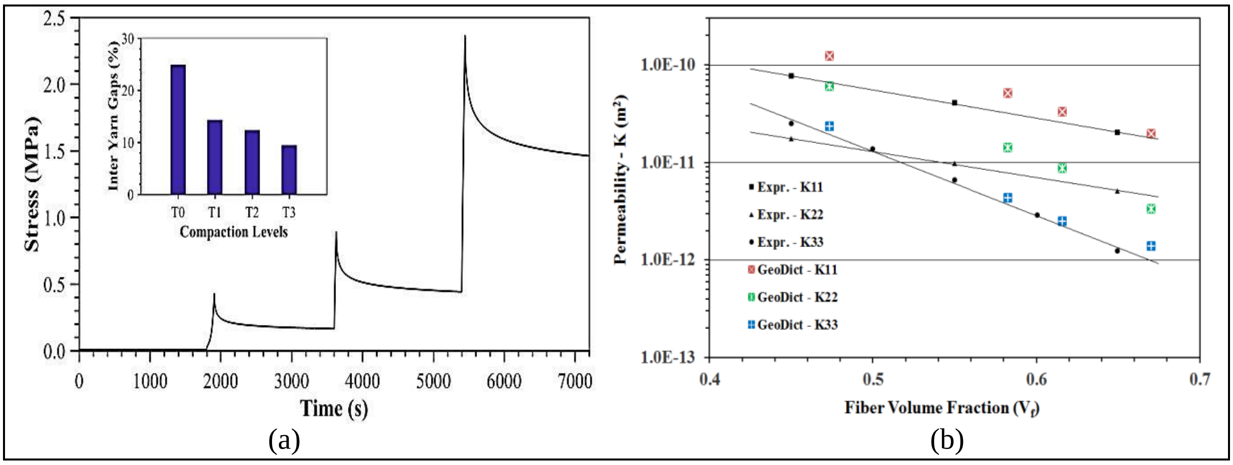

Figure 2: *(a) The multi-stage relaxation curve and (b) principle permeabilities (computed and experimental results).*

Conclusion

A novel non-destructive method to compute the preform permeability using real-time 3D fabric microstructure model generated from computed tomographic images has been successfully presented. Using the 3D reconstructed geometry, the permeabilities of an orthogonal 3D fabric at different fibre volume fractions were computed through two different numerical simulation packages. The results were in very good agreement with the experimental data.

References

[1] P. Boisse, *Composite reinforcements for optimum performance*: Cambridge : Woodhead, 2011., 2011.

[2] N. Vernet, E. Ruiz, S. Advani, *et al.*, "Experimental determination of the permeability of engineering textiles: Benchmark II," *Composites Part A: Applied Science and Manufacturing*, vol. 61, pp. 172-184, 2014.

[3] M. A. Ali, R. Umer, K. A. Khan, *et al.*, "Graphene coated piezo-resistive fabrics for liquid composite molding process monitoring," *Composites Science and Technology*, vol. 148, pp. 106-114, 8/18/ 2017.

[4] A. R. Aziz, M. A. Ali, X. Zeng, *et al.*, "Transverse permeability of dry fiber preforms manufactured by automated fiber placement," *Composites Science and Technology*, vol. 152, pp. 57-67, 2017.

[5] K. A. Khan and R. Umer, "Modeling the viscoelastic compaction response of 3D woven fabrics for liquid composite molding processes," *Journal of Reinforced Plastics and Composites*, 2017.

[6] H. Alhussein, R. Umer, S. Rao, *et al.*, "Characterization of 3D woven reinforcements for liquid composite molding processes," *Journal of Materials Science*, vol. 51, pp. 3277-3288, 2016.